

Quantifying global potential for coral evolutionary response to climate change

Cheryl A. Logan¹, John P. Dunne², James S. Ryan¹, Marissa L. Baskett³ and Simon D. Donner⁴

Incorporating species' ability to adaptively respond to climate change is critical for robustly predicting persistence. One such example could be the adaptive role of algal symbionts in setting coral thermal tolerance under global warming and ocean acidification. Using a global ecological and evolutionary model of competing branching and mounding coral morphotypes, we show symbiont shuffling (towards taxa with increased heat tolerance) was more effective than symbiont evolution in delaying coral-cover declines, but stronger warming rates (high emissions scenarios) outpace the ability of these adaptive processes and limit coral persistence. Acidification has a small impact on reef degradation rates relative to warming. Global patterns in coral reef vulnerability to climate are sensitive to the interaction of warming rate and adaptive capacity and cannot be predicted by either factor alone. Overall, our results show how models of spatially resolved adaptive mechanisms can inform conservation decisions.

nthropogenic climate change is affecting marine ecosystems worldwide¹ and accelerating the rate of species extinctions^{2,3}. Range shifts and rapid adaptation can circumvent this risk⁴, but sessile species with low adaptive capacity are among those most threatened⁵. Incorporating adaptive capacity (for example, due to genetics or acclimatization) into models of population size and geographic distribution can better predict climate change effects on species survival and ecosystem function^{4,6,7}.

Mechanistic predictions of adaptive capacity at a global scale can indicate where adaptation most affects future predictions^{4,6}. Accounting for adaptive capacity might then shift expectations about overall vulnerability and where climate impacts might be greatest^{8,9}, which can inform conservation priorities¹⁰. For example, locations projected to experience greater future climate variability and extremes might be expected to also experience the greatest impacts. Yet species in these same locations might undergo selection for higher heat tolerance and therefore have greater adaptive capacity to warming. Given these contrasting possibilities, accounting for both evolutionary dynamics and climate stress can inform which locations might require more protection^{9,11}.

Coral reefs provide a model system for exploring interactions between adaptive capacity and vulnerability to climate stress. Corals are economically and ecologically important foundational species that have already experienced climate-driven losses¹². Under moderate emissions scenarios, global models suggest corals will experience bleaching more frequently than anticipated recovery rates by mid-century^{13–15}, although few have explicitly considered adaptive capacity (but see refs. ^{16–20}). Another challenge for predicting coral vulnerability is understanding the potential interactive effects of temperature with ocean acidification (OA), which can impede coral skeletal growth¹⁵. Coral growth and thermal tolerance are greatly affected by endosymbiotic photosynthetic microalgae²¹, and symbiont-mediated adaptive capacity may enable corals to rapidly respond to warming. With large population sizes, high genetic diversity and short generation times,

symbionts have high adaptive potential^{22–24}, and shuffling towards more heat-tolerant taxa has been shown to increase bleaching thresholds by up to 1.5 °C over ecological timescales^{25,26}. Modelling the extent to which natural adaptive processes can increase heat tolerance is critical for making conservation decisions, especially as potentially risky human interventions are considered (for example, assisted migration)^{27,28}.

In this article, we quantitatively assess the effect of symbiont-mediated adaptive capacity using a global ecological and evolutionary model capable of simulating coral responses to warming and OA. Our model (Extended Data Fig. 1) includes two ecologically realistic coral morphotypes²⁹ that compete for space: (1) a competitive, faster-growing, heat-sensitive branching coral relative to a (2) slower-growing, heat-tolerant mounding coral. We assume coral growth and thermal tolerance are emergent properties of symbiont population size and thermal characteristics²¹. Symbiont genotypes determine thermal optima, while the coral host determines sensitivity to temperature departures from that optimum, with initial symbiont genotypes matched to local thermal history. We simulate symbiont-mediated adaptive capacity in both coral morphotypes through (1) natural selection of symbiont populations (evolution²²⁻²⁴) and (2) shifts between heat-sensitive and heat-tolerant symbiont communities ('shuffling'25,26). Evolution is simulated using a quantitative genetic model, which results in thermal tolerance increases of 0.3-1.8°C depending on climate scenario and reef location. Shuffling is simulated by addition of a heat-tolerant symbiont population with a thermal growth optimum +0.5, 1 or 1.5 °C above that of a heat-sensitive symbiont population²⁶ that becomes competitively superior under warming. We also estimate potential effects of OA on coral growth on the basis of changes in aragonite saturation³⁰. To characterize regions where adaptive capacity most alters expectations about relative climate impacts, we apply the model to projected monthly sea surface temperatures (SSTs) in 1,925 reef cells for four representative concentration pathways (RCP 2.6, 4.5, 6.0 and 8.5) through 2100.

¹Department of Marine Science, California State University, Monterey Bay, Seaside, CA, USA. ²NOAA/OAR Geophysical Fluid Dynamics Laboratory, Princeton, NJ, USA. ³Department of Environmental Science and Policy, University of California Davis, Davis, CA, USA. ⁴Department of Geography, University of British Columbia, Vancouver, British Columbia, Canada. [⊠]e-mail: clogan@csumb.edu

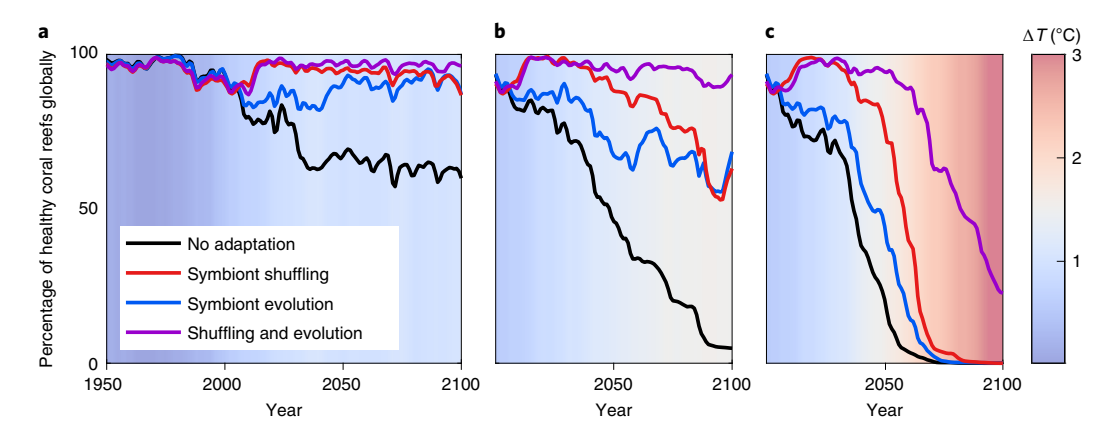


Fig. 1 | Percentage of 'healthy' reef cells globally in three RCP emissions scenarios from 1950 to 2100. Model trajectories are shown with no adaptation (black), symbiont shuffling with a +1 °C advantage (red), symbiont evolution (blue), and combined shuffling and evolution (purple). A reef is considered healthy if it is not in a bleached or mortality state (Methods). Background colour represents the average increase in annual maximum temperatures relative to the historical average from 1860 to 2000 across all reef grid cells. **a**, RCP 2.6. **b**, RCP 4.5. **c**, RCP 8.5.

| Table 1 Global coral health metrics at 2100 in simulations with and without adaptive capacity | | | | | | | | | | | | |
|---|----------------------|--------------|----------------|---------------------------|--------------|----------------|--------------------|--------------|----------------|--------------------------------|--------------|----------------|
| | No adaptive capacity | | | Symbiont shuffling (+1°C) | | | Symbiont evolution | | | Shuffling (+1°C) and evolution | | |
| RCP | % Cover | % Healthy | % Branching | % Cover | % Healthy | % Branching | % Cover | % Healthy | % Branching | % Cover | % Healthy | % Branching |
| 2.6 | 37 | 57 | 2 | 65 | 85 | 56 | 81 | 84 | 61 | 72 | 96 | 71 |
| 4.5 | 3 | 5 | 0 | 28 | 65 | 20 | 41 | 71 | 18 | 65 | 94 | 62 |
| 6.0 | 1 | 1 | 0 | 5 | 21 | 1 | 7 | 21 | 0 | 58 | 90 | 57 |
| 8.5 | 1 | 0 | 0 | 1 | 0 | 0 | 1 | 0 | 0 | 10 | 23 | 13 |

For each simulation and RCP, relative coral extent ('% Cover') reported as percentage of a pre-warming fixed carrying capacity in each reef cell, percentage of reef cells not bleached or dead ('% Healthy') and percentage of reef cells where branching (heat-sensitive) corals ('% Branching') are the dominant coral morphotype are reported.

The global model supported coexistence of mounding and branching coral populations at steady state between 1861 and 1950, before major anthropogenic warming, given our parameterization for interspecific competition. In simulations where the anthropogenic signal was removed, both morphotypes coexisted through 2300, regardless of starting proportions (Extended Data Fig. 2). At steady state, branching corals made up ~90% of total carrying capacity and mounding corals filled ~1%. To quantify changes in coral cover in simulations with and without adaptive capacity, we examined how relative coral extent varies through time. Relative coral extent is defined here as the percentage of a fixed pre-warming carrying capacity made up by both coral morphotypes in each reef cell and averaged across all cells (weighted equally). Actual available coral habitat varies widely by reef, so relative extent does not directly correlate with geographic extent.

In baseline model runs (no adaptive capacity), relative coral extent was ≤3% by 2100 under all climate scenarios except RCP 2.6 (37%) (Table 1). In these RCPs, most reef cells either had experienced ≥2 bleaching events in the previous decade or were dead (such reef cells are hereafter referred to as 'degraded'; Methods), reaching degradation rates >95% by 2100 (Fig. 1 and Extended Data Fig. 3, black lines). We define bleaching as a decrease in symbiont density below 30% of the minimum symbiont population size in the previous year (Extended Data Fig. 4). Although end-of-century degradation rates were lower in RCP 2.6 (43%), 98% of reef cells were composed of only mounding corals, following a shift from branching to mounding communities in the 2040s across all RCPs (Fig. 2, top row). Sensitivity analyses show that coral persistence is enhanced if the model is calibrated to a lower 1985–2010 global

bleaching frequency but that relative differences among adaptive mechanisms remain the same (Extended Data Fig. 5).

Effects of symbiont-mediated adaptive capacity

Symbiont shuffling leading to higher thermal tolerance (+1 °C) substantially delayed or prevented widespread mortality by 2100, with the largest differences in RCP 4.5 (Figs. 1 and 2). In RCP 2.6, shuffling averted mid-century population declines and a shift towards mounding coral communities (Fig. 2). By contrast, shuffling had little effect in RCP 6.0 and RCP 8.5 by 2100 (Table 1), with relative coral extent remaining \leq 5%. Shuffling to symbionts with even higher tolerance (+1.5°C) increased relative coral extent to 58% for RCP 6.0 by 2100, but remained ≤3% for RCP 8.5 (Supplementary Table 1). Shuffling to symbionts with lower tolerance (+0.5 °C) had little effect on relative coral extent at 2100 (≤2% for all RCPs except RCP 2.6) (Supplementary Table 1). Fidelity to heat-tolerant symbionts occurred in both coral morphotypes between 2010 and 2025 in most reef cells (Extended Data Fig. 6). Complete transitions to heat-tolerant symbiont communities often occurred in under 5-10 years as warming rates increased, although coexistence and reversion to heat-sensitive symbionts is possible in the model (Extended Data Fig. 7).

Symbiont evolution resulted in thermal tolerance increases of 0.3–1.8 °C depending on climate scenario and reef location (Extended Data Fig. 8). Evolution delayed degradation most under RCP 4.5 and RCP 6.0 but had little effect on relative coral extent under RCP 8.5 (Figs. 1 and 2). Relative coral extent increased most under RCP 4.5, from 3% to 41% by 2100 (Table 1), and degradation was delayed by ~50 years (Fig. 1b). By 2100, however, mounding

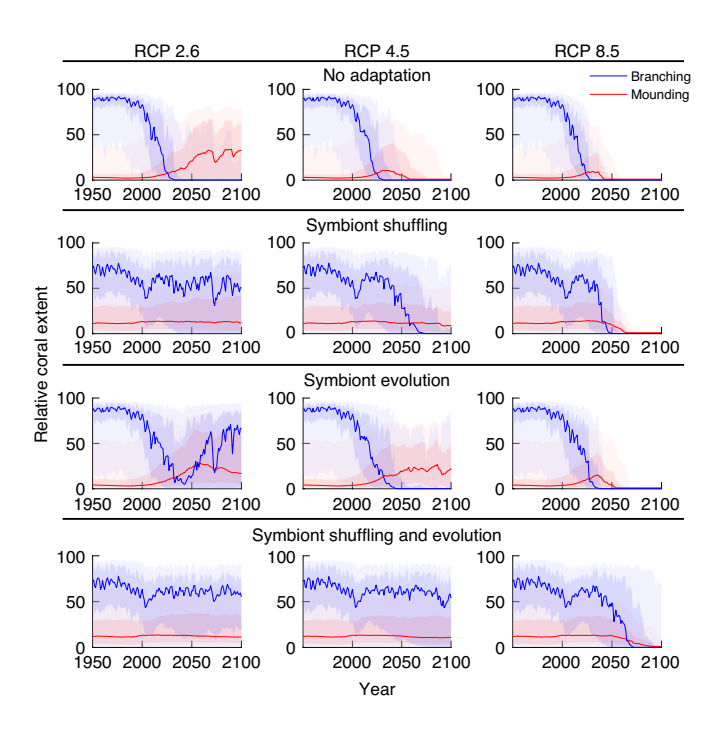


Fig. 2 | Relative coral extent with and without symbiont-mediated adaptive capacity. Mean, quartile and 5th to 95th percentiles across all reef cells (n = 1,925) for branching (heat-sensitive) corals and mounding (heat-tolerant) corals as a percentage of a fixed pre-warming carrying capacity averaged across all reef cells. Panels show simulations with no adaptation (top row), with symbiont shuffling only (+1 °C advantage) (second row), with symbiont evolution only (third row) and with combined shuffling and evolution (bottom row). Columns correspond to low (RCP 2.6), moderate (RCP 4.5) and high (RCP 8.5) emissions scenarios.

coral populations became dominant in most reef cells (Fig. 2). Under RCP 2.6, evolution increased relative coral extent from 37% to 81% (Table 1), and branching corals remained dominant in most reef cells by 2100, albeit with large mid-century population declines (Fig. 2, third row). Compared with shuffling (+1 $^{\circ}$ C), evolution was less effective in averting decline of coral populations under all RCPs (Figs. 1 and 2).

In model runs where shuffling (+1 °C) and evolution occurred concurrently, coral persistence dramatically increased in RCP 4.5, RCP 6.0 and RCP 8.5 (Fig. 1). These simulations show similar mid-century trends to shuffling only, but evolution continues to increase thermal tolerance through 2100. Relative coral extent was ≥58% by 2100 in all RCPs except RCP 8.5, where it remained 10% (Table 1). Only simulations where both shuffling (+1.5 °C) and evolution co-occur enabled moderate coral persistence by 2100 under RCP 8.5 (47% relative coral extent) (Supplementary Table 1).

To examine how adaptive capacity altered expectations for relative vulnerability across locations, we compared the last year in which reef cells avoided degradation under RCP 4.5 with that in RCP 8.5 (Fig. 3). In the baseline model, degradation occurred earliest in the Red Sea, the Persian Gulf and the western equatorial Pacific (Fig. 3a,b). Coral persistence was higher in the central Pacific and near Malaysia and western Indonesia. Shuffling (+1 °C) slowed rates of degradation in the central Pacific and Coral Triangle under RCP 8.5 (Fig. 3d,b), areas with both lower projected warming and less SST variability (Extended Data Fig. 9b,j). Under RCP 4.5, shuffling had a stronger global effect compared with baseline, except in high-latitude areas with higher seasonal variability (for example, northern Red Sea, East China Sea) and locations projected to have high interannual maximum SST variability (for example,

southern Caribbean, equatorial Pacific) (Extended Data Fig. 9e,f). Evolution showed similar geographic patterns as for shuffling under RCP 4.5. Exceptions include parts of the Caribbean, where evolution increased persistence only near the Greater Antilles (Fig. 3e) in relation to relatively lower projected warming (Extended Data Fig. 9a,b) and SST variability (Extended Data Fig. 9i,j). Under RCP 8.5, evolution had a small effect compared with baseline model runs (Fig. 3f,b) with no apparent refugia emerging, although global degradation rates were delayed ~5–10 years. In simulations with combined evolution and shuffling (+1°C), most reef cells within the western and central Pacific survived through 2080 under RCP 4.5 and RCP 8.5 (Fig. 3g,h).

To evaluate environmental predictors of modelled extinction risk, we compared model vulnerability maps (Fig. 3) with global maps of warming rate and SST standard deviation (Extended Data Fig. 9), but none was a consistent indicator of vulnerability across locations. Correlations were highest between relative coral extent and future SST variation (all months) in shuffling runs, with R^2 ranging from 0.41 to 0.55; all other SST metrics and simulations had average R^2 values <0.2 (Supplementary Table 4).

Effects of ocean acidification

In simulations where OA negatively affected coral growth, coral degradation was greater across all reef cells, but not by more than 5% in any year (Extended Data Fig. 5). This effect was greatest when warming drove moderate reef mortality. For example, in RCP 8.5, OA increased the percentage of degraded reefs from 55.7% to 58.6% by 2050. Before 2020, when many reefs were still healthy, and after 2070, when mortality was high, OA had little effect on growth rate.

Discussion

Our results demonstrate that incorporating species' ability to adaptively respond to climate change is critical for robust, global-scale predictions of species' future persistence and extent. Model simulations without adaptation predicted coral persistence through 2100 only under RCP 2.6 (Figs. 1 and 2), similar to previous threshold-based global-scale bleaching models^{13–15}. Symbiont-mediated adaptive capacity substantially altered coral population trajectories under low and moderate warming scenarios but had little effect under RCP 8.5. Shuffling was generally more effective than evolution in delaying coral-cover declines and shifts towards mounding coral communities (Figs. 1 and 2). Under RCP 8.5, the only simulation with >1% of healthy reef cells by 2100 included both symbiont evolution and shuffling, resulting in a relative coral extent of 10% (Table 1).

These results expand on previous studies^{16,17,19} to demonstrate how adaptive mechanisms can increase coral persistence under low-to-moderate, but not severe, climate change. We found that when shuffling increased thermal tolerance by +1 °C, coral persistence increased more than with evolution alone (Figs.1 and 2). The more-rapid shuffling mechanism has its largest impact between 2010 and 2040 (Extended Data Fig. 6) whereas evolution occurs at a slower rate but over a longer duration (Extended Data Fig. 8). Under RCP 8.5, adaptation delayed complete coral mortality by less than a decade but did not affect century-scale outcomes. Symbiont-mediated adaptive processes acting concurrently substantially prolonged coral survival under RCP 4.5 and RCP 6.0 with minimal shifts in coral community composition (Fig. 2).

Coral community shifts described here have been reported in the field following bleaching events³¹ but have not previously been globally projected. From an ecological perspective, community shifts are likely to compromise reef structural complexity and long-term stability of reef-associated biodiversity³². We found that shifts towards mounding coral communities began earlier with evolution than with shuffling (Fig. 2), further demonstrating how these mechanisms result in different outcomes. Shuffling maximizes thermal tolerance in most reefs by 2040, after which time both coral

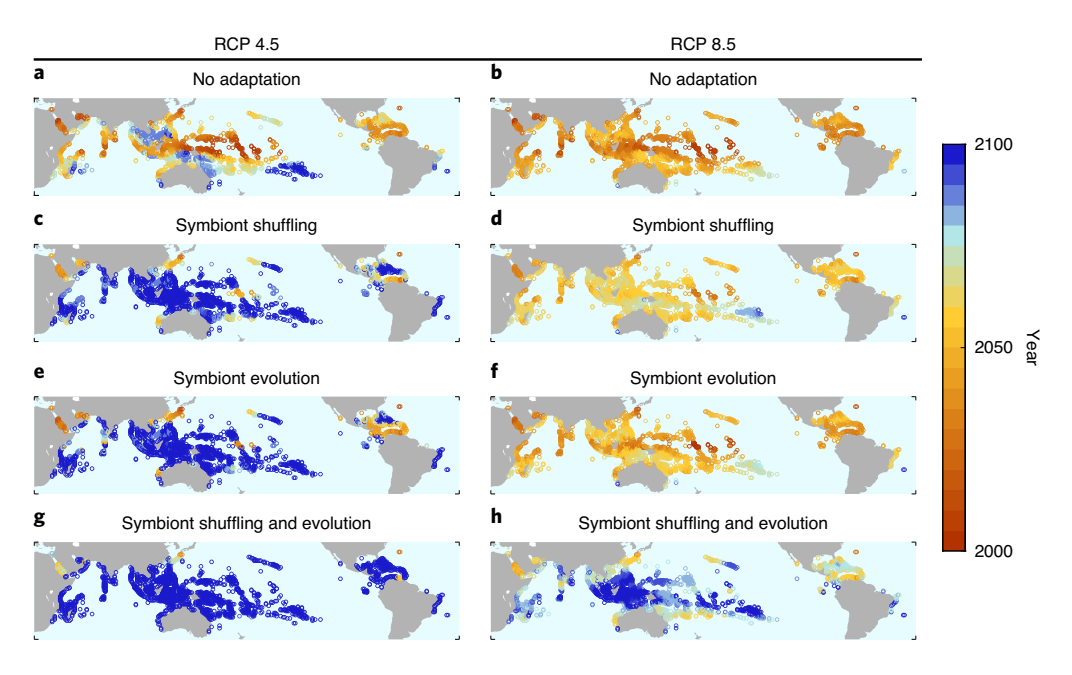


Fig. 3 | Maps depicting the last year at which corals are projected to survive before the onset of high-frequency bleaching (≥2 events within the previous decade) or mortality. a-h, Model output is shown with no adaptation (a,b), symbiont shuffling with a +1°C advantage (c,d), symbiont evolution (e,f) or both shuffling and evolution (g,h) under moderate (RCP 4.5) (a,c,e,g) and high (RCP 8.5) (b,d,f,h) emissions scenarios. Reef cells in the darkest blue are projected to have some coral cover beyond 2100.

morphotypes exhibit fidelity to heat-tolerant symbionts (Extended Data Fig. 6), as has been observed in some of the hottest reefs in the world³³. We also identified scenarios where adaptive capacity enabled coral communities to shift back to baseline when warming rates declined (for example, RCP 2.6 with evolution; Fig. 2). Although this trajectory would be possible only under conditions not fully considered in our model (adequate recruitment, available substrate and reduction of local stressors), it suggests adaptive mechanisms may enable some reefs to retain present-day structure and function under RCP 2.6.

Previous work has suggested only a minor additional impact of OA on coral persistence compared with warming 14, with benefits of higher-latitude thermal refugia largely offset by relatively lower aragonite saturation (Ω) values 15. Our results suggest an even lower OA sensitivity with an attributable global reduction of coral persistence to OA of <5% (Extended Data Fig. 5). This agreement suggests that effects of OA through Ω -reduced bleaching thresholds and Ω -reduced growth rates are minor compared with warming. However, modelling including substrate strength effects found a 70% drop in coral cover with a doubling of atmospheric CO₂ 34. Thus, OA influences through Ω effects on bleaching susceptibility and substrate strength may play a much more important role than through reductions in growth rate included in the present study.

Our model identifies regions where adaptation alters expectations about where climate impacts are highest. In some cases, we found that relative vulnerability was similar with and without adaptation. For example, higher-latitude reef cells with higher seasonal variability were among the most vulnerable locations regardless of adaptation under RCP 4.5 (Fig. 3, left panels). Yet in other regions, relative vulnerability differed when adaptive capacity was included. In the Coral Triangle, most reefs persisted through 2100 with adaptation in RCP 4.5, whereas large portions were among the most vulnerable with no adaptation. Geographic patterns of persistence were somewhat similar between evolution and shuffling, with some key exceptions. For example, shuffling is projected to increase persistence across the entire Caribbean region under RCP 4.5, whereas evolution enabled long-term persistence only in reef cells where

both warming magnitude and SST variation is projected to be relatively lower (Extended Data Fig. 9a,i). Under RCP 8.5 (Fig. 3, right panels), evolution had little effect, but shuffling enabled reefs in the central South Pacific and central Coral Triangle to persist 20–25 years in relation to relatively less projected warming and SST variability (Extended Data Fig. 9b,j).

Given the threat to coral reefs even with <1.5 °C of global warming³⁵, research is increasingly focusing on identifying conservation priorities. Overall, the results highlight that such research, typically based on current reef status and response to past disturbances³⁶, should include relative future warming and adaptive potential. For example, Walsworth et al.¹¹ found that optimal management strategies focus on coral thermal refugia in models without adaptation, but prioritizing trait and habitat diversity or high cover is more effective in models with adaptation. We also show that geographic patterns in model results depend on adaptive mechanism modelled (Fig. 3), and areas predicted to be more vulnerable on the basis of change in SST or SST variation alone did not always predict vulnerability (Extended Data Fig. 9). Other adaptive mechanisms not simulated here may produce different geographic patterns of persistence and vulnerability.

Like all models, our simplistic representation of coral reef ecology and evolution introduces several uncertainties and biases that might affect our results. Abiotic and biotic factors not included here, including light, sea-level rise, storm damage, pollution, overfishing, herbivory, coral disease and competition for space with other organisms, might lead us to overestimate coral persistence and recovery37. Factors that might lead us to underestimate likelihood of persistence include other mechanisms of adaptation³⁸ (for example, coral-host adaptation/acclimatization or epigenetics) and gene flow^{17,18,39}. In addition, while coarse resolution SSTs can capture average bleaching incidence across locations⁴⁰, bleaching incidence will further depend on local-scale factors such as high-frequency temperature variation and depth, which are potential mitigators of bleaching⁴¹. Climate-model downscaling would be needed to inform local-scale management decisions. Furthermore, models with different climate sensitivity⁴² and climate variability (for example, El Niño/Southern Oscillation) may give quantitatively different results. In addition,

uncertain model parameters could lead to over- or underestimation of coral persistence. Selectional variance (symbiont thermal tolerance breadth) was the most sensitive parameter in a sensitivity analysis completed on a regional version of this model¹⁹. In our study, selectional variance was calibrated to reef cell thermal history and historical global bleaching frequencies. Future studies could include revised estimates of past bleaching events.

Our model also highlights research avenues that could improve our understanding of symbiont-mediated adaptive processes. First, the prevalence of shuffling across coral taxa in wild populations remains unclear. Although multiple symbiont types have been detected at low abundance in most coral taxa examined⁴³, not all corals have the flexibility to shuffle^{33,44-46}. Second, the degree to which symbiont thermal tolerance can evolve and confer coral-host tolerance in the wild is unknown. Heat-evolved Symbiodiniaceae lab strains have shown increased growth at temperatures 1–4 °C above ambient temperatures after 40–120 generations, but these gains did not always increase coral heat tolerance^{24,47}. Finally, more empirical measurements of time-dependent thermal performance curves⁴⁸ for both coral and symbiont growth would improve our ability to model population growth dynamics.

Due to recent increases in mass bleaching events worldwide¹², the management community is evaluating human interventions that may increase the persistence of coral reefs^{27,28}. If the 2015 Paris Agreement upper goal of limiting warming to less than 2°C is reached, this would align most closely with RCP 2.6. Under this scenario, symbiont-mediated increases in thermal tolerance might enable corals to survive through 2100 without drastic shifts in coral community composition. Under RCP 4.5, evolution and shuffling could improve projections of coral cover and degradation rates. However, under RCP 6.0 and 8.5, coral-dominated communities as we know them today are expected to essentially disappear. As managers and decision makers consider human interventions to increase thermal tolerance or decrease local thermal stress²⁷, assessing existing potential natural adaptive capacity using mechanistic models could help inform decisions²⁸.

Online content

Any methods, additional references, Nature Research reporting summaries, source data, extended data, supplementary information, acknowledgements, peer review information; details of author contributions and competing interests; and statements of data and code availability are available at https://doi.org/10.1038/s41558-021-01037-2.

Received: 4 February 2020; Accepted: 31 March 2021; Published online: 17 May 2021

References

- IPCC Special Report on the Ocean and Cryosphere in a Changing Climate (eds Pörtner, H.-O. et al.) (IPCC, 2019).
- Urban, M. C. Accelerating extinction risk from climate change. Science 348, 571–573 (2015).
- McCauley, D. J. & Pinsky, M. L. Marine defaunation: animal loss in the global ocean. Science 347, 1255641 (2015).
- 4. Hoffmann, A. A. & Sgrò, C. M. Climate change and evolutionary adaptation.
- Nature 470, 479–485 (2011).
 5. Somero, G. N. The physiology of climate change: how potentials for acclimatization and genetic adaptation will determine 'winners' and 'losers'.
- J. Exp. Biol. 213, 912–920 (2010).
 Kearney, M. & Porter, W. Mechanistic niche modelling: combining physiological and spatial data to predict species' ranges. Ecol. Lett. 12, 334–350 (2009).
- Foden, W. B. et al. Identifying the world's most climate change vulnerable species: a systematic trait-based assessment of all birds, amphibians and corals. PLoS ONE 8, e65427 (2013).
- West, J. M. & Salm, R. V. Resistance and resilience to coral bleaching: implications for coral reef conservation and management. *Conserv. Biol.* 17, 956–967 (2003).

Baskett, M. L., Nisbet, R. M., Kappel, C. V., Mumby, P. J. & Gaines, S. D.
Conservation management approaches to protecting the capacity for corals to
respond to climate change: a theoretical comparison. *Glob. Change Biol.* 16,
1229–1246 (2010).

- Beyer, H. L. et al. Risk-sensitive planning for conserving coral reefs under rapid climate change. Conserv. Lett. 11, e12587 (2018).
- Walsworth, T. E. et al. Management for network diversity speeds evolutionary adaptation to climate change. Nat. Clim. Change 9, 632–636 (2019).
- Hughes, T. P. et al. Spatial and temporal patterns of mass bleaching of corals in the Anthropocene. Science 359, 80–83 (2018).
- Donner, S. D., Skirving, W. J., Little, C. M., Oppenheimer, M. & Hoegh-Guldberg, O. Global assessment of coral bleaching and required rates of adaptation under climate change. *Glob. Change Biol.* 11, 2251–2265 (2005).
- Frieler, K. et al. Limiting global warming to 2°C is unlikely to save most coral reefs. Nat. Clim. Change 3, 165–170 (2012).
- Van Hooidonk, R., Maynard, J. A., Manzello, D. & Planes, S. Opposite latitudinal gradients in projected ocean acidification and bleaching impacts on coral reefs. *Glob. Change Biol.* 20, 103–112 (2014).
- Logan, C. A., Dunne, J. P., Eakin, C. M. & Donner, S. D. Incorporating adaptive responses into future projections of coral bleaching. *Glob. Change Biol.* 20, 125–139 (2014).
- Bay, R. A., Rose, N. H., Logan, C. A. & Palumbi, S. R. Genomic models predict successful coral adaptation if future ocean warming rates are reduced. Sci. Adv. 3, e1701413 (2017).
- Matz, M. V., Treml, E. A. & Haller, B. C. Estimating the potential for coral adaptation to global warming across the Indo-West Pacific. *Glob. Change Biol.* 26, 3473–3481 (2020).
- Baskett, M. L., Gaines, S. D. & Nisbet, R. M. Symbiont diversity may help coral reefs survive moderate climate change. Ecol. Appl. 19, 3–17 (2009).
- Matz, M. V., Treml, E. A., Aglyamova, G. V. & Bay, L. K. Potential and limits for rapid genetic adaptation to warming in a Great Barrier Reef coral. PLoS Genet. 14, e1007220 (2018).
- Muscatine, L., Falkowski, P. G., Porter, J. W. & Dubinsky, Z. Fate of photosynthetic fixed carbon in light- and shade-adapted colonies of the symbiotic coral Stylophora pistillata. Proc. R. Soc. Lond. B. 222, 181–202 (1984).
- Csaszar, N. B., Ralph, P. J., Frankham, R., Berkelmans, R. & van Oppen, M. J. Estimating the potential for adaptation of corals to climate warming. PLoS ONE 5, e9751 (2010).
- Howells, E. J. et al. Coral thermal tolerance shaped by local adaptation of photosymbionts. Nat. Clim. Change 2, 116–120 (2012).
- Buerger, P. et al. Heat-evolved microalgal symbionts increase coral bleaching tolerance. Sci. Adv. 6, eaba2498 (2020).
- Baker, A. C. Flexibility and specificity in coral-algal symbiosis: diversity, ecology, and biogeography of Symbiodinium. Annu. Rev. Ecol. Evol. Syst. 34, 661–689 (2003).
- Berkelmans, R. & van van Oppen, M. J. H. The role of zooxanthellae in the thermal tolerance of corals: a 'nugget of hope' for coral reefs in an era of climate change. *Proc. R. Soc. Lond. B* 273, 2305–2312 (2006).
- National Academies of Sciences, Engineering, and Medicine A research
 Review of Interventions to Increase the Persistence and Resilience of Coral Reefs
 (National Academies Press, 2019).
- National Academies of Sciences, Engineering, and Medicine A Decision
 Framework for Interventions to Increase the Persistence and Resilience of Coral
 Reefs (National Academies Press, 2019).
- Darling, E. S., Alvarez-Filip, L., Oliver, T. A., McClanahan, T. R. & Côté, I. M. Evaluating life-history strategies of reef corals from species traits. *Ecol. Lett.* 15, 1378–1386 (2012).
- Chan, N. C. S. & Connolly, S. R. Sensitivity of coral calcification to ocean acidification: a meta-analysis. Glob. Change Biol. 19, 282–290 (2013).
- Hughes, T. P. et al. Global warming transforms coral reef assemblages. Nature 556, 492–496 (2018).
- 32. Darling, E. S. et al. Relationships between structural complexity, coral traits, and reef fish assemblages. *Coral Reefs* **36**, 561–575 (2017).
- Howells, E. J. et al. Corals in the hottest reefs in the world exhibit symbiont fidelity not flexibility. Mol. Ecol. 29, 899–911 (2020).
- Madin, J. S., Hughes, T. P. & Connolly, S. R. Calcification, storm damage and population resilience of tabular corals under climate change. *PLoS ONE* 7, e46637 (2012).
- 35. Hoegh-Guldberg, O. et al. in *Global Warming of 1.5°C* (eds Masson-Delmotte, V. et al.) Ch. 3 (IPCC, 2018).
- Darling, E. S. et al. Social–environmental drivers inform strategic management of coral reefs in the Anthropocene. Nat. Ecol. Evol. 3, 1341–1350 (2019).
- Wilkinson, C. R. Global and local threats to coral reef functioning and existence: review and predictions. Mar. Freshw. Res. 50, 867–878 (1999).
- Palumbi, S. R., Barshis, D. J., Traylor-Knowles, N. & Bay, R. A. Mechanisms of reef coral resistance to future climate change. Science 344, 895–898 (2014).
- Kleypas, J. A. et al. Larval connectivity across temperature gradients and its potential effect on heat tolerance in coral populations. *Glob. Change Biol.* 22, 3539–3549 (2016).

- Heron, S. F. et al. Validation of reef-scale thermal stress satellite products for coral bleaching monitoring. *Remote Sens.* 8, 59 (2016).
- 41. Safaie, A. et al. High frequency temperature variability reduces the risk of coral bleaching. *Nat. Commun.* **9**, 1671 (2018).
- Forster, P. M. et al. Evaluating adjusted forcing and model spread for historical and future scenarios in the CMIP5 generation of climate models. J. Geophys. Res. Atmos. 118, 1139–1150 (2013).
- 43. Ziegler, M., Eguíluz, V. & Duarte, C. et al. Rare symbionts may contribute to the resilience of coral–algal assemblages. *ISME J* 12, 161–172 (2018).
- Sampayo, E. M., Ridgway, T., Bongaerts, P. & Hoegh-Guldberg, O. Bleaching susceptibility and mortality of corals are determined by fine-scale differences in symbiont type. *Proc. Natl Acad. Sci. USA* 105, 10444–10449 (2008).
- 45. Thornhill, D. J., Xiang, Y. U., Fitt, W. K. & Santos, S. R. Reef endemism, host specificity and temporal stability in populations of symbiotic dinoflagellates from two ecologically dominant Caribbean corals. *PLoS ONE* 4, e6262 (2009).
- 46. Stat, M., Loh, W. K. W., LaJeunesse, T. C., Hoegh-Guldberg, O. & Carter, D. A. Stability of coral–endosymbiont associations during and after a thermal stress event in the southern Great Barrier Reef. *Coral Reefs* 28, 709–713 (2009).
- Chakravarti, L. J., Beltran, V. H. & van Oppen, M. J. Rapid thermal adaptation in photosymbionts of reef-building corals. *Glob. Change Biol.* 23, 4675–4688 (2017).
- Schulte, P. M., Healy, T. M. & Fangue, N. A. Thermal performance curves, phenotypic plasticity, and the time scales of temperature exposure. *Integr. Comp. Biol.* 51, 691–702 (2011).

Publisher's note Springer Nature remains neutral with regard to jurisdictional claims in published maps and institutional affiliations.

© The Author(s), under exclusive licence to Springer Nature Limited 2021

Methods

We scaled and modified a coral-symbiont eco-evolutionary model originally described in ref. ¹⁹ to the global level. Here we provide a description of the model (Extended Data Fig. 1) and modifications made to globalize the model and incorporate potential effects of ocean acidification.

Coral population dynamics and parameters. The model follows area cover for two coral morphotypes, a heat-tolerant slow-growing mounding type ($C_{\rm M}$) and a heat-sensitive fast-growing branching type (C_B) (Extended Data Fig. 1 and equations (1-6)). These traits are generally based on those associated with common mounding and branching morphotypes, respectively⁴⁹. Coral thermal tolerance depends on symbiont populations whose genotypes determine the thermal optimum (Symbiont population dynamics and parameters). Corals compete for space in a closed system using Lotka-Volterra dynamics with a competition factor α_{mn} (the competitive effect of coral n on coral m) and a fixed carrying capacity (K_{C_m}) that varies by coral type m (M or B). Branching corals are more competitive than mounding corals as in ref. 50. Carrying capacity was determined on the basis of area occupied by each morphotype (to report coral cover in cm²) and multiplied by a conversion constant from projected area to total surface area51. Coral growth rates decline linearly with increasing coral density to represent coral density dependence. Growth rates increase linearly with symbiont density (S_{im} relative to symbiont carrying capacity per unit of coral density $K_{S_{im}}$) to represent corals' dependence on symbionts for carbon^{29,52}, up to a coral-specific maximum growth rate of γ_m based on ref. 53. The model assumes that symbiont density is within a range such that increases in symbiont densities lead to increased coral carbon acquisition and growth 54,55. Coral basal mortality rates are fixed (μ) in the absence of symbionts with parameters based on refs. 51,56 and decrease as symbiont density increases. Mortality rates exceed growth rates when symbiont density is ~0.5 × 106 cells cm⁻² (a density where bleaching has been observed in the field⁵⁷) and are represented in the model by u_m , the influence of symbiont density on coral mortality. In simulations with ocean acidification, we multiply coral growth by the coral calcification rate f (see Ocean acidification below).

All coral parameters $(K_{C_m}, \alpha_{mn}, \gamma_m, \mu_m, u_m)$ vary by coral type m, with branching corals (C_B) having a higher fixed carrying capacity (K_{C_m}) , a greater competitive ability (α_{mn}) , a faster growth rate (γ_m) , higher basal mortality in the absence of symbionts (μ_m) and a lower value for the influence of symbionts on mortality (u_m) (Supplementary Table 2 and references therein). Coral population dynamics are:

$$\frac{\mathrm{d}C_m}{\mathrm{d}t} = C_m \left[\frac{f^2 \gamma_m \frac{\sum_i S_{mm}}{K_{S_m} C_m}}{K_{C_m}} \left(K_{C_m} - \sum_n \alpha_{mn} C_n \right) - \frac{\mu_m}{1 + u_m \frac{\sum_i S_{mm}}{K_{S_m} C_m}} \right]. \tag{1}$$

Symbiont population dynamics and parameters. We follow symbiont population size S_{im} as the number of cells of symbiont type i in coral type m (cells cm $^{-2}$ of coral) (Extended Data Fig. 1 and equation (2)). Density dependence regulates symbiont density in each coral. Total symbiont carrying capacity per unit area, K_{S_m} , is proportional to C_m , the three-dimensional coral surface area and based on peak values for symbiont densities described in ref. 57 . Symbiont carrying capacity is independent of genotype and scaled by the maximum symbiont population growth rate $\hat{r}(t)$ such that the symbiont type with the greater population growth rate, $r_{im}(t)$, is competitively superior. In other words, because we scale competition between symbiont types by growth rate, relative growth for a given temperature determines the competitive outcome. The temperature-dependent maximum symbiont population growth rate function, $\hat{r}(t) = ae^{b\theta(t)}$, is based on the Eppley equation, where a and b are constants found for phytoplankton and e is Euler's number e0. Symbiont population dynamics, e1, of symbiont type e2 or e3 in coral type e3. Symbiont population dynamics, e5, of symbiont type e6 or e7 in coral type e9.

$$\frac{\mathrm{d}S_{im}}{\mathrm{d}t} = \frac{S_{im}}{K_{S_m}C_m} \left[r_{im}(t)K_{S_m}C_m - \hat{r}(t) \sum_j S_{jm} \right],\tag{2}$$

where $\sum_{i} S_{jm}$, sums the cells for all symbiont types in coral type m. Symbiont

populations grow on the basis of the difference between their thermal tolerance phenotype and the temperature $\theta(t)$ (which varies with time t) according to a temperature-dependent exponential growth rate equation derived from phytoplankton growth rate is similar to the value reported from phytoplankton growth rate is similar to the value reported from phytoplankton growth rate is similar to the value reported which has from ref. The width of this thermal tolerance function, thermal tolerance breadth σ_{wm}^2 , depends on coral type m and is inversely related to selection strength in simulations with evolution. Thermal tolerance breadth varies by coral host to allow greater thermal tolerance (slower drop-off in growth with temperature departures from the symbiont-genotype-determined optimum) in mounding versus branching coral morphotypes (for example, due to coral morphology or physiology) through differential susceptibility of each coral's symbionts to thermal stress. Symbiont populations have thermal tolerance phenotypes (temperature at peak performance) normally distributed around mean genotype \bar{g}_{im} with environmental variance σ_e^2 (described in the following). Thermal tolerance genotypes also follow a normal

distribution with mean $\bar{g}_{im}(t)$ and variance $\sigma^2_{gim}(t)$, both of which are constant in simulations without evolution and vary in time for evolution model runs. The overall population growth rate $r_{im}(t)$ for symbiont population i in coral host m is:

$$r_{im}(t) = \left\{ 1 - \frac{\sigma_{gim}^2(t) + \sigma_c^2 + \left[\min\left(\mathbf{L}_{\overline{g}_{im}}(t) - \theta(t) \right) \right]^2}{2\sigma_{wm}^2} \right\} \times ae^{b\left[\theta(t) - 2 \times \min\left(0, \theta(t) - \overline{g}_{im}(t) + L \right) \right]}$$
(3)

Following this equation, symbiont growth rate ($r_{im}(t)$) decreases at temperatures higher or lower than the optimum, with steeper declines occurring at temperatures above the optimum for growth rate. This modified version of the equation from ref. ¹⁹ includes a minimum function so that a rapid drop in symbiont growth rate applies only when temperatures are higher than symbionts' adapted genotype, thus avoiding unrealistic cold-water mortality events before the onset of 20th-century warming. The minimum function varies with thermal tolerance breadth where $L = \sqrt{2.6\sigma_{wm}^2}$. Negative population growth rates indicate that mortality rate exceeds reproduction rate and can disrupt symbiosis and lead to bleaching. Symbiont populations have an initial mean thermal tolerance phenotype and genotype $\bar{g}_{im}(0)$ equal to mean historical SST in each reef grid cell between 1861 and 2000. Thermal tolerance breadth σ_{wm}^2 is proportional to variance in historical monthly SST between January 1861 and December 2001 and assumes that corals living in more-variable thermal environments have greater capacity to withstand larger thermal fluctuations.

Symbiont genetic dynamics. In evolution simulations, we model symbiont thermal tolerance as a haploid quantitative genetic trait using a continuous time approach. The 'thermal tolerance phenotype' (described in the preceding) is the temperature to which a single symbiont population is adapted in each of the two coral morphotypes and on the basis of its mean population genotype. For each symbiont population i in coral m, the population genotype is modelled as a normal distribution with a mean genotype \bar{g}_{im} and, for models with evolution, genetic variance of σ^2_{eim} (Extended Data Fig. 1 and equations (4) and (5)). The phenotype varies around the genotype with random environmental variance σ^2_e (fraction of variation not due to heritability). Heritability (h^2) of thermal tolerance was estimated to be 0.330, an estimate for typical physiological traits. Heritability estimates of coral thermal tolerance driven by symbionts have been found to range between 0.23 and 0.5 12 . Environmental variance σ^2_e was calculated as the fraction of total phenotypic variation (σ^2_p) not explained by h^2 , such that $\sigma^2_e = (1-h^2) \times (\sigma^2_p)$. The mean genotype dynamics are:

$$\frac{\mathrm{d}\bar{g}_{im}}{\mathrm{d}t} = \frac{\sigma_{gim}^{2}(t) \left[\theta(t) - \bar{g}_{im}(t)\right]}{\sigma_{wm}^{2}} a \mathrm{e}^{b\theta(t)}.$$
 (4)

Within a population, genetic diversity can increase through new mutations and decrease through selection. In the model, mutation increases genetic variation at a constant rate of $\sigma_{\rm M}^2$. Mutational variance is calculated as $\sigma_{\rm M}^2 = \sigma_{\rm e}^2 \times 0.001 \, {\rm yr}^1$ as in ref. 19 and on the basis of reported values for the ratio $\sigma_{\rm M}^2/\sigma_{\rm e}^2$ as 0.0001–0.05 per generation for a variety of model organisms 61 and on the approximate symbiont generation time of 0.2 years 21 . The model assumes that stabilizing selection occurs for the optimal phenotype and is represented by selectional variance (σ_{wm}^2) , or thermal tolerance breadth, which is inversely related to selection strength. Selectional variance is proportional to the width of the symbiont population growth rate (fitness) function. The genetic variance dynamics are:

$$\frac{\mathrm{d}\sigma_{gim}^2}{\mathrm{d}t} = \sigma_{\mathrm{M}}^2 - \frac{\sigma_{gim}^4(t)}{\sigma_{um}^2} a \mathrm{e}^{b\theta(t)}.$$
 (5)

Values for all symbiont parameters (K_{S_m} , a, b, $\sigma_{\rm e}^2$, $\sigma_{\rm M}^2$, σ_{wm}^2) are based on ref. ¹⁹ and references therein (Supplementary Table 2).

Finally, we set the selectional variance (σ_{wm}^2 ; width of the fitness function or thermal tolerance breadth) to be proportional to the historical mean and variance in each reef cell using a proportionality constant, ρ . In the absence of precise global bleaching records available to 'tune' the model to each individual reef cell's bleaching history, we applied a heuristic approach at the global scale to define ρ . Similar to our previous study¹⁶, we modified ρ to result in a global bleaching frequency of 3 or 5% between 1985 and 2010 (x% of the reef cells bleach, on average, in a given year). The accurate global bleaching frequency during this time frame is not knowable, but these bleaching frequencies are within the range of realistic possibilities on the basis of extrapolation from a high-resolution global bleaching database⁶² and fall within the range of annual severe bleaching occurrences across 100 regions between 1985 and 2010 (ref. 12). The proportionality constant (ρ) was defined for each reef cell on the basis of the ratio between the historical (1861-2000) mean and variance of the exponential term of Eppley's equation⁵⁸ (e^{0.0633T}) to capture physiological effects of temperature variability across time and space:

$$\rho = \frac{1}{s} \left[\frac{\text{mean} \left(e^{bT} \right)}{\text{var} \left(e^{bT} \right)} \right]^{y}.$$

Empirical values s and y remain constant across all reefs for any given RCP, but s varies with each adaptation simulation (for example, baseline, shuffling and evolution) to tune the global bleaching frequency to the historical bleaching target (Supplementary Table 3). The proportionality constant assumes a greater physiological effect of temperature variability at high than low temperatures, with the physiological effects of temperature variability depending on the kinetics of activation energy which, for many organic reactions, follow the Eppley exponential curve **. We then constrain the proportionality constant to between 0.5 and 1.50 to best match the targeted global bleaching frequency between 1985 and 2010. To determine selectional variance (σ^2_{wm}), or thermal tolerance breadth, the proportionality constant is then multiplied by the historical temperature variance in each cell. For mounding corals, σ^2_{wm} is then increased by 25%, which provides a wider thermal tolerance range compared with branching (heat-sensitive) corals.

Symbiont shuffling. To simulate symbiont shuffling as a result of symbiont diversity, simulations begin with two symbiont populations in each coral type (evolution-only simulations include only one symbiont population). The additional population begins as a low-abundance heat-tolerant symbiont type (for example, genus Durusdinium). Heat-tolerant symbionts have an initial thermal optimum (\bar{g}_{2m}) of +0.5, 1, or 1.5 °C above that of the heat-sensitive symbionts, enabling them to grow faster as temperature increases. The symbiont population growth rate (r_{im}) is calculated from the mean genotype \bar{g}_{im} , so the symbiont growth rates are different between the two symbiont types, with heat-tolerant symbionts having a higher maximum growth rate according to the Eppley function. Density dependence within and between symbiont populations regulates symbiont density in each coral morphotype at a level proportional to $C_{\rm M}$ given total symbiont carrying capacity per unit area K_{S_m} . Density dependence is scaled by the maximum possible population growth rate $\hat{r}(t)$ so that symbionts with the greater population growth rate $r_{im}(t)$ under a given temperature at time t are competitively superior. The model includes also a trade-off for hosting heat-tolerant symbionts, where corals hosts are penalized with up to a 50% decrease in coral growth rate (similar to ref. 63). The growth penalty is proportional to the percentage of heat-tolerant symbionts in each coral and applied by multiplying the coral growth rate (λ_m) by this weighted value after each time step. If temperature decreases, the heat-sensitive symbiont type can re-populate the coral, removing both the thermal advantage and the coral growth penalty. The goal was to simulate symbiont community shifts due to heat-tolerant symbionts being present in low abundance that could become dominant after bleaching⁶⁴. Our model also assumes a trade-off between growth rate and thermal tolerance such that competition between the symbiont populations depends on temperature (symbionts with the greater population growth rate $r_{im}(t)$ are competitively superior). To test the effect of symbiont evolution in combination with shuffling, we also included model runs with and without evolution of both symbiont types.

Ocean acidification. To test the effect of OA on coral growth rate, we used a relationship between $\Omega_{\rm Arag}$ and coral calcification rate (f) previously described³⁰, where a 0.15 slope represents the mean sensitivity of coral calcification to $\Omega_{\rm Arag}$ across multiple coral taxa:

$$f(\Omega_{\text{Arag}}) = 1 - 0.15 (4 - \Omega_{\text{Arag}}) \text{ where } 1 \le \Omega_{\text{Arag}} \le 4.$$
 (6)

On the basis of equation (6), Ω_{Arag} values were calculated for each reef cell for all four RCPs (National Oceanic and Atmospheric Administration (NOAA) Geophysical Fluid Dynamics Laboratory Earth system model 2 M (ESM2M)^{65,66}). For Ω_{Arag} values below one, the factor is set to zero, and for values above four, the factor is set to one. For OA model runs, this function was included in the equation for the coral growth rate (equation (1)). The value of f is squared because calcification rate correlates with linear growth rates f, but coral population size is estimated from total coral surface area calculated in two dimensions.

Model application. The model applies differential equations for coral and symbiont growth, competition and genetic adaptation of symbionts, which are integrated forward in time using a second-order Runge–Kutta method in Matlab (R2019b; MathWorks). We scaled this model to 1,925 reef-containing grid cells, identified by projecting the Millennium Coral Reef Mapping Project⁶⁸ map of coral reefs to the grid used by the NOAA Geophysical Fluid Dynamics Laboratory ESM2M⁶⁵. To validate coexistence of the coral morphotypes in the absence of an anthropogenic warming signal, we executed the model from 1861 to 2300 with no warming (Extended Data Fig. 2). The model was then executed from 1861 to 2100 using bias-corrected monthly SST output from ESM2M for each of the four RCP Intergovernmental Panel on Climate Change Fifth Assessment Report warming scenarios^{16,65}, using a time step of 0.125 months. Combining a heuristic model, at the scale of a coral, with projected climate-model resolution is justified on the basis of the ability of coarse thermal stress data to predict the likelihood of bleaching⁶⁰; this approach has been used in previous coral-modelling studies^{9,13–18}.

Model output analysis (bleaching, mortality and recovery definitions). For the purposes of visualizing model output for each model year, reef cells are categorized as being healthy, bleached or frequently bleached (\geq 2 events within the previous

decade), or in a mortality state (Extended Data Fig. 4). However, this heuristic model implementation is not intended to make absolute predictions of coral cover, bleaching or mortality for individual reefs. Instead, it is calibrated to give zero mortality by 1950 and 3% or 5% bleaching per reef cell per year on average between 1985 and 2010. This approximation to actual conditions allows the model to represent the effect of alternative climate scenarios and other conditions. For these purposes, 'bleaching' events are defined by comparing the minimum annual symbiont density in each reef cell with the previous year. By defining bleaching events, we can compare the results with previous threshold-based models 13,1 Bleaching events herein are defined when symbiont density decreases below 30% of the minimum symbiont population size in the previous year on the basis of data showing that visible severe bleaching can occur even when corals retain between 20% and 50% of their original algal population 70. This definition was developed to capture warm-water bleaching events, but cold-water bleaching can occur⁷¹. Reef cells also enter a bleached state when bleaching occurs ≥2 times in the previous decade (similar to ref. 13). If either coral type bleaches in a given year, the reef cell enters a 'bleached state'. A single reef cell can bleach only once per year.

Following bleaching, a reef cell can remain bleached, transition to a state of mortality or recover to a healthy state (Extended Data Fig. 4). A mortality state is defined for a reef cell when a coral population declines below twice its seed value, regardless of symbiont density. A reef cell also enters a state of mortality if it does not recover within 5 years after bleaching. Although it is not ecologically realistic for a reef to remain bleached for more than a few weeks to months, this categorization allowed us to differentiate between short- and long-term bleaching effects. To include the potential for recovery following bleaching or mortality, but in the absence of data to explicitly model connectivity between reefs globally, a small 'seed' population of corals and symbionts is included at all time steps to represent resupply of larvae from source populations. For mounding and branching coral morphotypes, respectively, the seed population sizes are 1% and 0.1% of carrying capacity, which assumes mounding (heat-tolerant) corals are ten times more abundant than branching (heat-sensitive) corals following a bleaching or mortality event⁴⁹. For symbionts, the seed density is 0.00001% of carrying capacity, calculated with the conservative assumption that coral population size is at its seed value. In model runs with evolution, seed symbionts are assumed to be adapted to temperature changes through time. For recovery to occur, both coral and symbiont populations must grow to at least four times their respective seed values. In addition, because coral growth can slowly increase despite fluctuations in symbiont population size, recovery is also defined when a coral population grows to >10% of carrying capacity.

Vulnerability maps based on warming rates and temperature variability. To compare predicted regions of vulnerability on the basis of SST changes alone with model results, we produced maps based on temperature metrics expected to trigger bleaching and mortality (Extended Data Fig. 9). These maps included five metrics: change in maximum monthly mean SST from the historical period (1861-1900) to 2080, change in SST variability from the historical period (1861-1900) to the period between 2050 and 2080 (maximum monthly mean, all months) and future SST variability between 2050 and 2080 (maximum monthly mean, all months) for RCP 4.5 and RCP 8.5. To evaluate these metrics as possible predictors of modelled extinction risk, we also compared each metric with relative coral extent using a least-squares linear regression across all combinations of evolution and shuffling simulations. The R² values were calculated each year between 2020 and 2060 using a sliding window for the future climatological period or year for all reef cells containing >5% relative coral extent and averaged over time. This time frame maximized the number of reef cells that could be used in the analysis, before extensive degradation in all simulations (Fig. 1).

Reporting Summary. Further information on research design is available in the Nature Research Reporting Summary linked to this article.

Code availability

All Matlab code can be found at https://github.com/VeloSteve/Coral-Model-V12 under the following: https://doi.org/10.5281/zenodo.2639126.

References

- Loya, Y. et al. Coral bleaching: the winners and the losers. Ecol. Lett. 4, 122–131 (2001).
- Langmead, O. & Sheppard, C. Coral reef community dynamics and disturbance: a simulation model. Ecol. Modell. 175, 271–290 (2004).
- Chancerelle, Y. Methods to estimate actual surface areas of scleractinian coral at the colony- and community-scale. Oceanol. Acta 23, 211–219 (2000).
- Falkowski, P. G., Dubinsky, Z., Muscatine, L. & Porter, J. W. Light and the bioenergetics of a symbiotic coral. *Bioscience* 34, 705–709 (1984).
- Huston, M. Variation in coral growth rates with depth at Discovery Bay, Jamaica. Coral Reefs 4, 19–25 (1985).
- Hoogenboom, M., Beraud, E. & Ferrier-Pagès, C. Relationship between symbiont density and photosynthetic carbon acquisition in the temperate coral Cladocora caespitosa. Coral Reefs 29, 21–29 (2010).

- Cunning, R. & Baker, A. C. Not just who, but how many: the importance of partner abundance in reef coral symbioses. Front. Microbiol. 5, 400 (2014).
- McClanahan, T., Muthiga, N. & Mangi, S. Coral and algal changes after the 1998 coral bleaching: interaction with reef management and herbivores on Kenyan reefs. Coral Reefs 19, 380–391 (2001).
- 57. Fitt, W. K., McFarland, F. K., Warner, M. E. & Chilcoat, G. C. Seasonal patterns of tissue biomass and densities of symbiotic dinoflagellates in reef corals and relation to coral bleaching. *Limnol. Oceanogr.* 45, 677–685 (2000).
- Eppley, R. W. Temperature and phytoplankton growth in the sea. Fish. Bull. 70, 1063–1085 (1972).
- Jon, N. Biodiversity and ecosystem functioning: a complex adaptive systems approach. *Limnol. Oceanogr.* 49, 1269–1277 (2004).
- Mousseau, T. A. & Roff, D. A. Natural selection and the heritability of fitness components. *Heredity* 59, 181–197 (1987).
- 61. Lynch, M. The rate of polygenic mutation. Genet. Res. 51, 137–148 (1988).
- Donner, S. D., Rickbeil, G. J. & Heron, S. F. A new, high-resolution global mass coral bleaching database. *PLoS ONE* 12, e0175490 (2017).
- Cunning, R., Gillette, P., Capo, T., Galvez, K. & Baker, A. C. Growth tradeoffs associated with thermotolerant symbionts in the coral *Pocillopora damicornis* are lost in warmer oceans. *Coral Reefs* 34, 155–160 (2015).
- Silverstein, R. N., Cunning, R. & Baker, A. C. Change in algal symbiont communities after bleaching, not prior heat exposure, increases heat tolerance of reef corals. *Glob. Change Biol.* 21, 236–249 (2015).
- Dunne, J. P. et al. GFDL's ESM2 global coupled climate–carbon Earth system models part I: physical formulation and baseline simulation characteristics. J. Clim. 25, 6646–6665 (2012).
- Dunne, J. P. et al. GFDL's ESM2 global coupled climate–carbon Earth system models Part II: carbon system formulation and baseline simulation characteristics. J. Clim. 26, 2247–2267 (2012).
- Lough, J. M. & Barnes, D. J. Environmental controls on growth of the massive coral *Porites. J. Exp. Mar. Biol. Ecol.* 245, 225–243 (2000).
- UNEP-WCMC, WorldFish Centre, WRI & TNC. Global Distribution of Warm-water Coral Reefs, Compiled From Multiple Sources Including the Millennium Coral Reef Mapping Project. Version 4.1 (UN Environment World Conservation Monitoring Centre. Data, 2021); https://doi.org/10.34892/ t2wk-5t34

- van Hooidonk, R., Maynard, J. A. & Planes, S. Temporary refugia for coral reefs in a warming world. Nat. Clim. Change 3, 508–511 (2013).
- Fitt, W., Brown, B., Warner, M. & Dunne, R. Coral bleaching: interpretation of thermal tolerance limits and thermal thresholds in tropical corals. *Coral Reefs* 20, 51–65 (2001).
- González-Espinosa, P. C. & Donner, S. D. Predicting cold-water bleaching in corals: role of temperature, and potential integration of light exposure. *Mar. Ecol. Prog. Ser.* 642, 133–146 (2020).

Acknowledgements

This work was supported by a NOAA Coral Reef Conservation grant to J.P.D. and S.D.D., a Coral Reef Alliance Coral Adaptation Challenge grant to C.A.L. and S.D.D., and an ROA supplement to NSF DEB #1655475 to C.A.L. and M.L.B. We thank C. M. Eakin for helpful initial discussions in the development of the global model. The contents in this manuscript are solely the opinions of the authors and do not constitute a statement of policy, decision or position on behalf of NOAA or the US Government.

Author contributions

C.A.L., J.P.D. and S.D.D. conceived and designed the global model; C.A.L. and J.S.R. developed and tested the computer code; C.A.L., J.P.D., J.S.R. and S.D.D. analysed the results; C.A.L. and J.S.R. wrote the paper. C.A.L., J.P.D., J.S.R., S.D.D. and M.L.B. critically revised the manuscript.

Competing interests

The authors declare no competing interests.

Additional information

Extended data is available for this paper at https://doi.org/10.1038/s41558-021-01037-2.

 $\label{thm:contains} \textbf{Supplementary information} \ The online version contains supplementary material available at $$https://doi.org/10.1038/s41558-021-01037-2.$

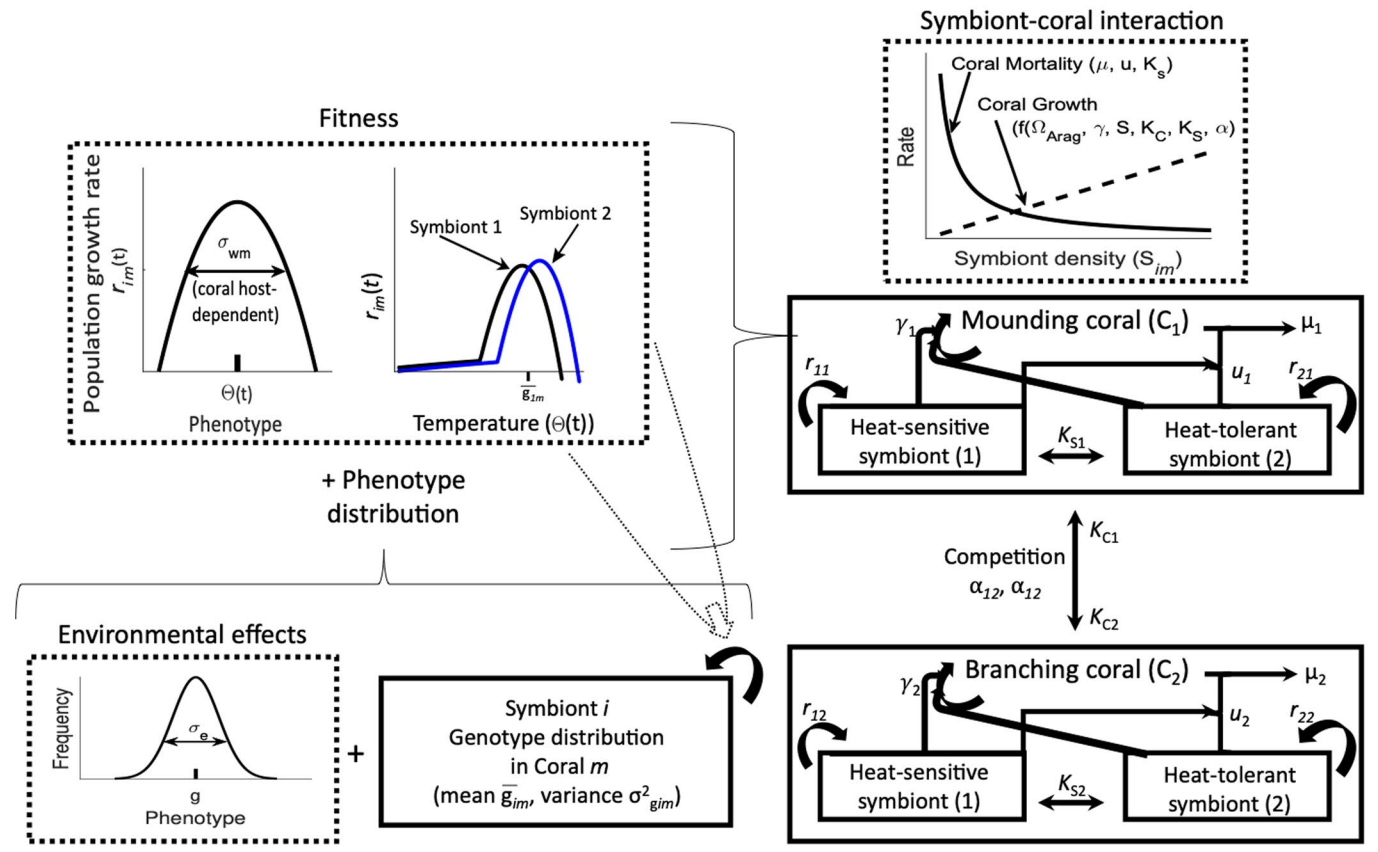
Correspondence and requests for materials should be addressed to C.A.L.

Peer review information *Nature Climate Change* thanks M. Matz and the other, anonymous, reviewer(s) for their contribution to the peer review of this work.

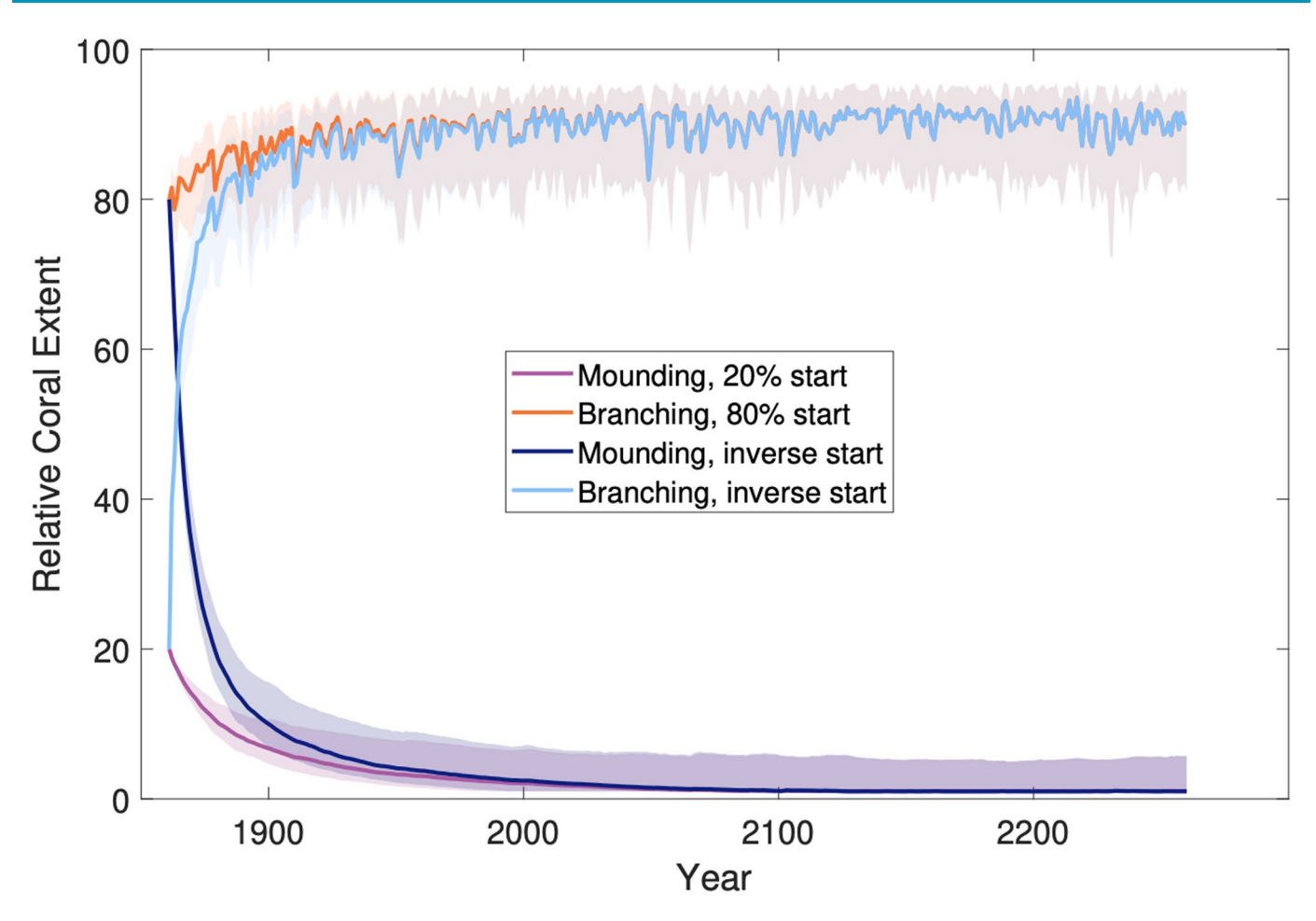
Reprints and permissions information is available at www.nature.com/reprints.

a) Symbiont genetic dynamics

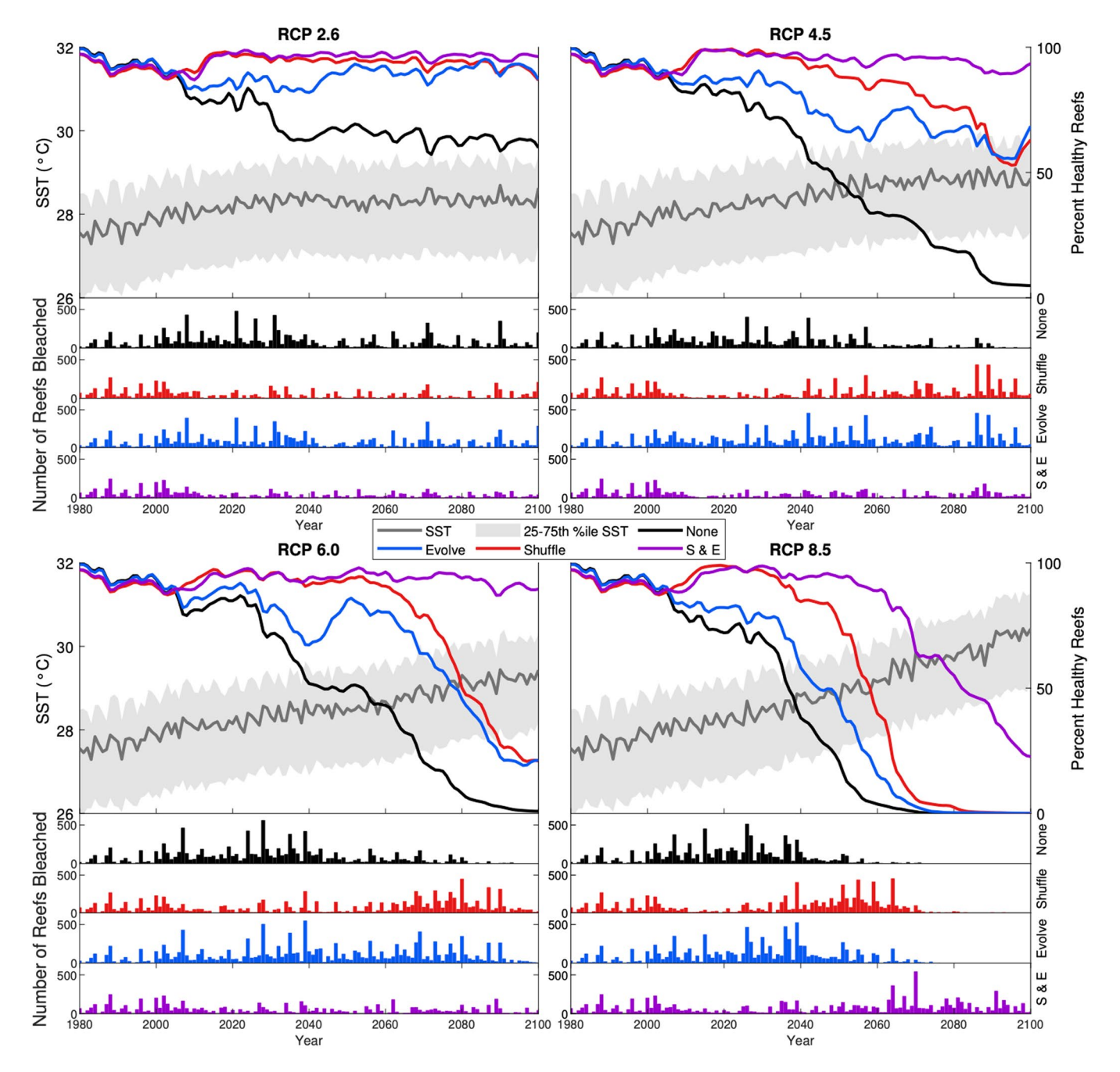
b) Coral and symbiont population dynamics



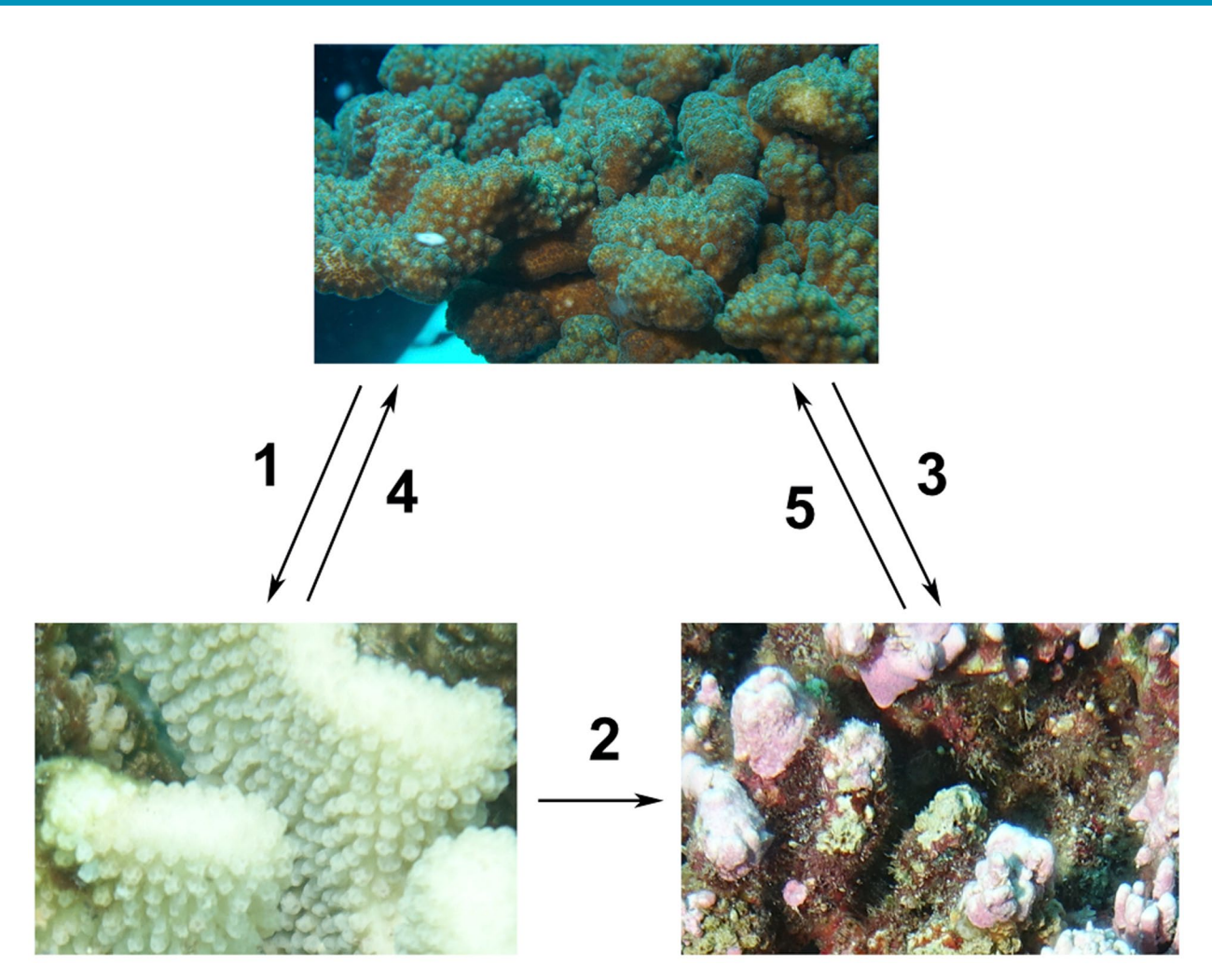
Extended Data Fig. 1 | Coral and symbiont ecological and evolutionary global model diagram. The left-hand boxes (**a**) describe the symbiont fitness curve and genetic dynamics. The right-hand boxes (**b**) describe the coral and symbiont population dynamics.



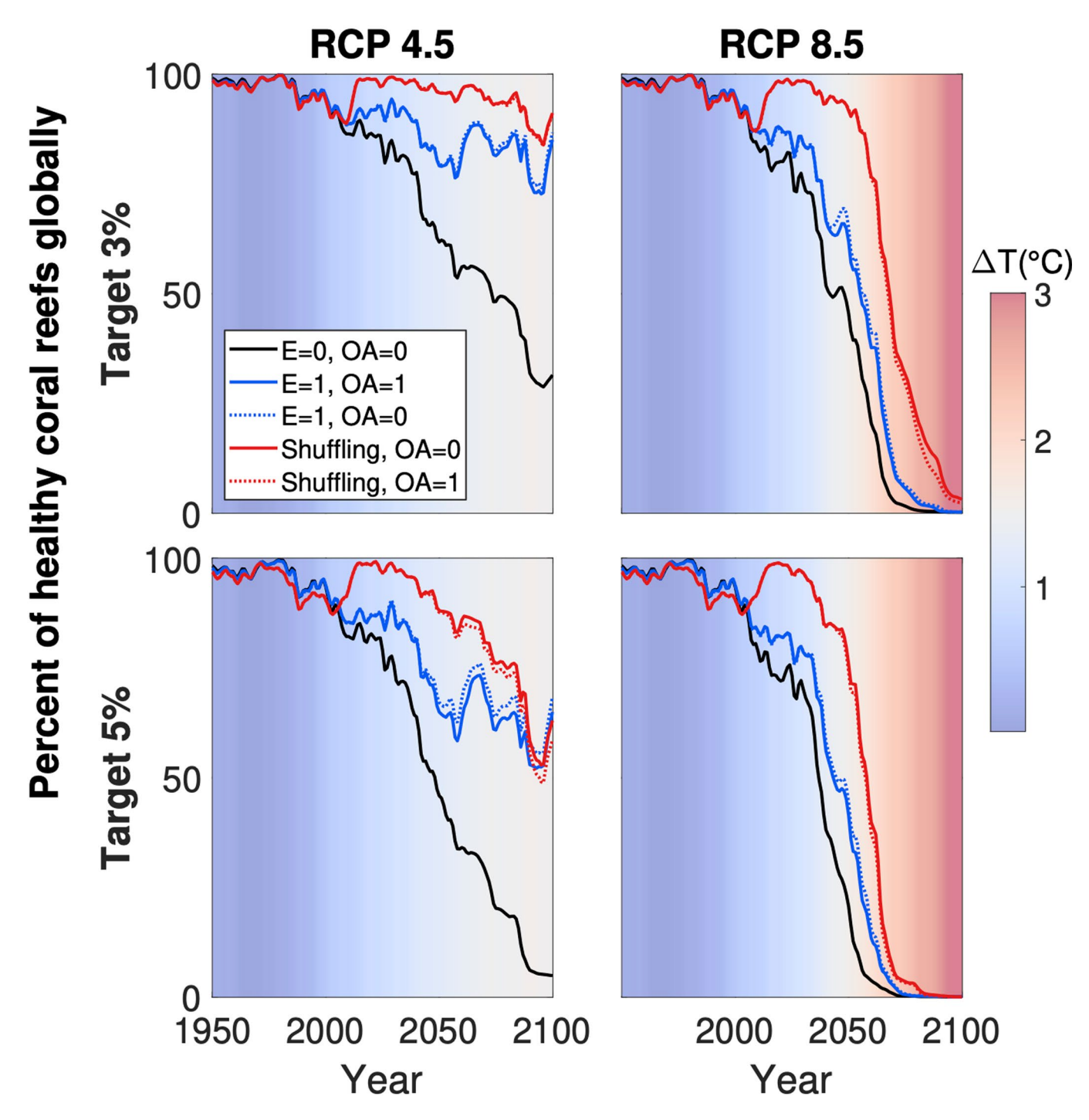
Extended Data Fig. 2 | Relative coral extent across all reef cells in a 400-year model run with no anthropogenic warming and no adaptive capacity. In all model runs, branching corals (blue) are initialized at 80% and mounding corals (red) at 20% of a fixed pre-warming carrying capacity (K) in 1861 averaged across all reef cells. Initializing coral morphotypes to the inverse of these proportions (80% mounding: 20% branching) results in a similar outcome (~90% branching and 1% mounding corals) by 1950. Shaded colors represent the 50% interquartile range around the mean for all reef cells.



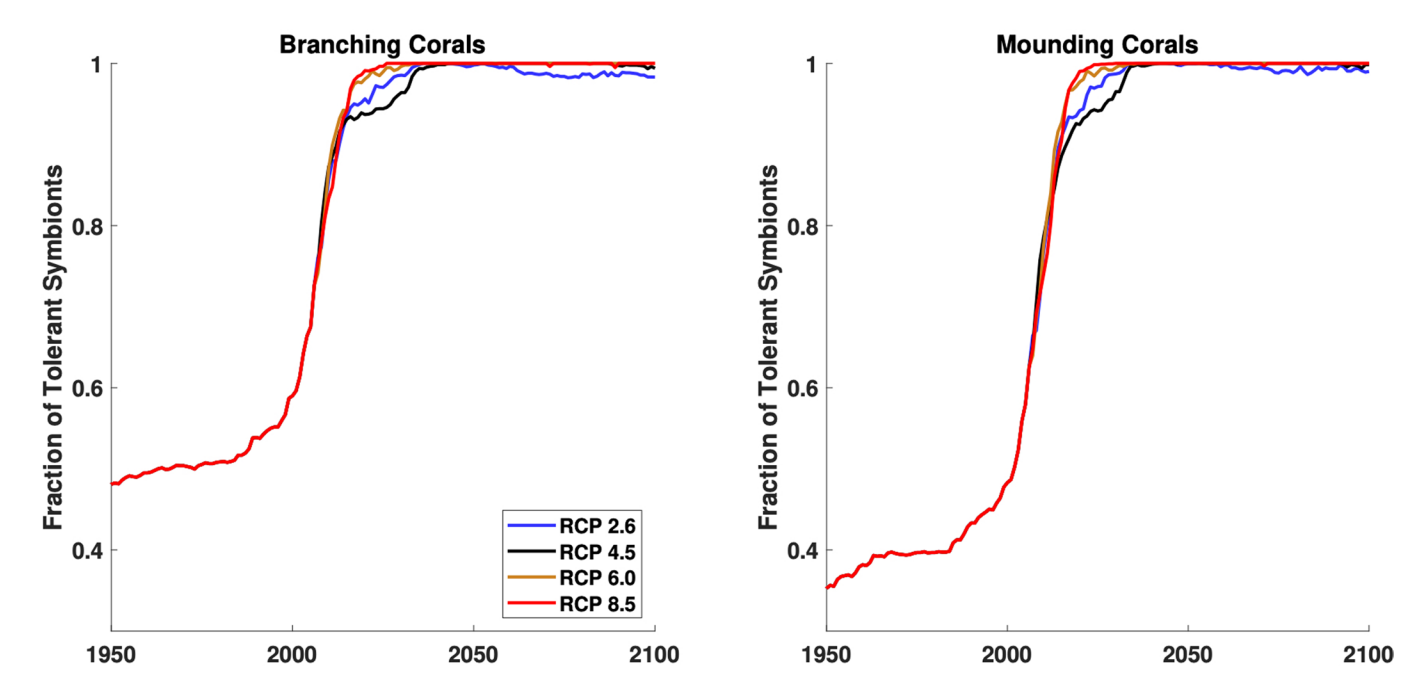
Extended Data Fig. 3 | Percentage of 'healthy' reef cells globally in four RCP emissions scenarios from 1980 to 2100. Model trajectories are shown with no evolution (black), shuffling with a +1°C advantage (red), evolution (blue), and combined shuffling and evolution (purple). A reef is considered 'healthy' if it is not in a bleached or mortality state (see Methods). SST (grey) is the mean and 25th-75th percentile increase in annual maximum temperatures across all reef grid cells. Bar plots indicate number of bleaching events per year in each model run.



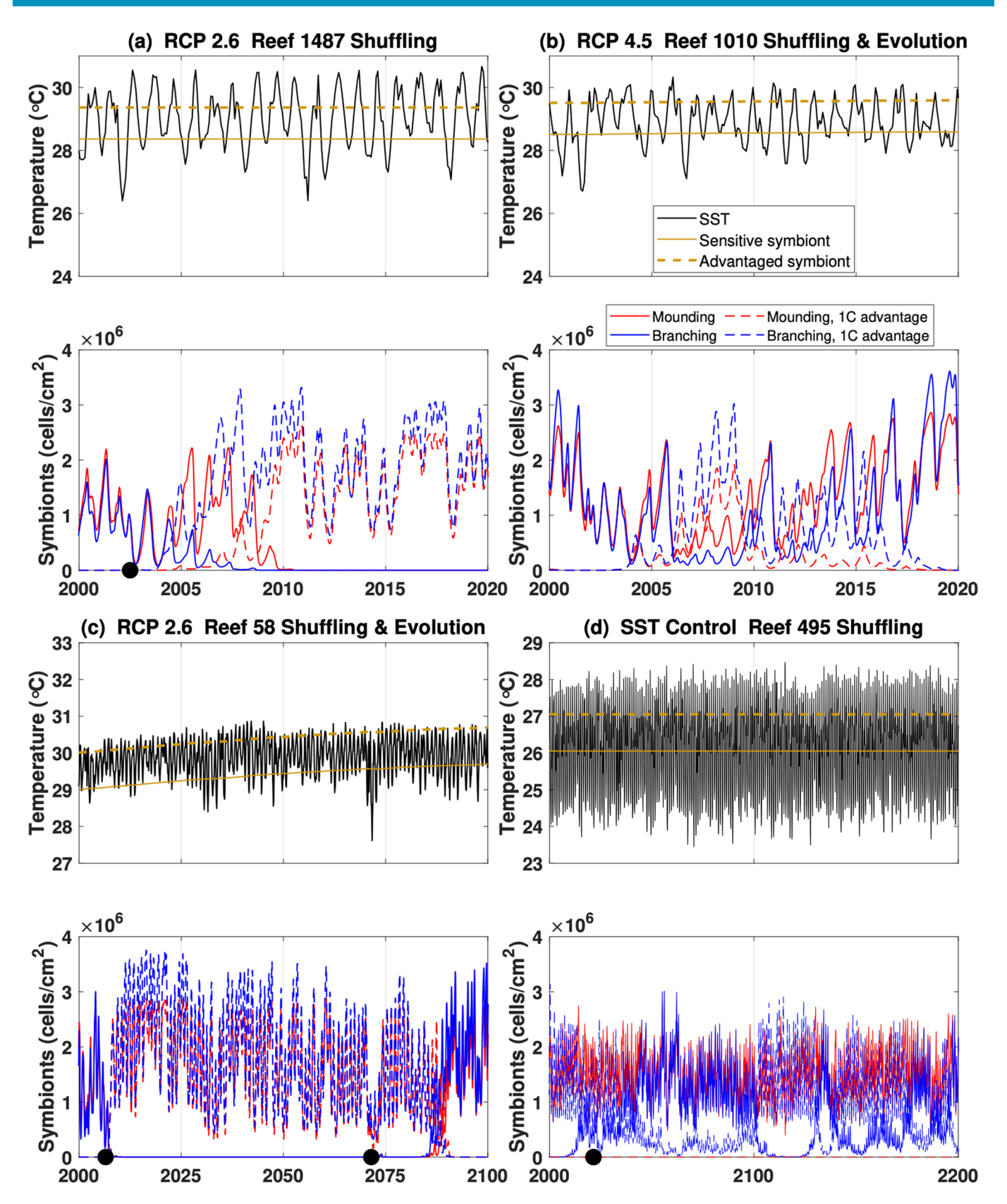
Extended Data Fig. 4 | In each model year, reef cells are defined as being in a 'healthy', 'bleached', or 'mortality' state. Arrows represent transitions between states. 1) 'Bleaching' occurs when symbiont populations drop <30% of the minimum population size in the previous year or when bleaching occurs ≥2 times in the previous decade. 2) 'Mortality' is defined if a reef bleaches but does not recover within five years, or 3) if coral populations drop to <2x the seed value. 4-5) Recovery occurs if coral and symbiont populations increase to >4x their respective seed value or coral populations grow above 10% of carrying capacity.



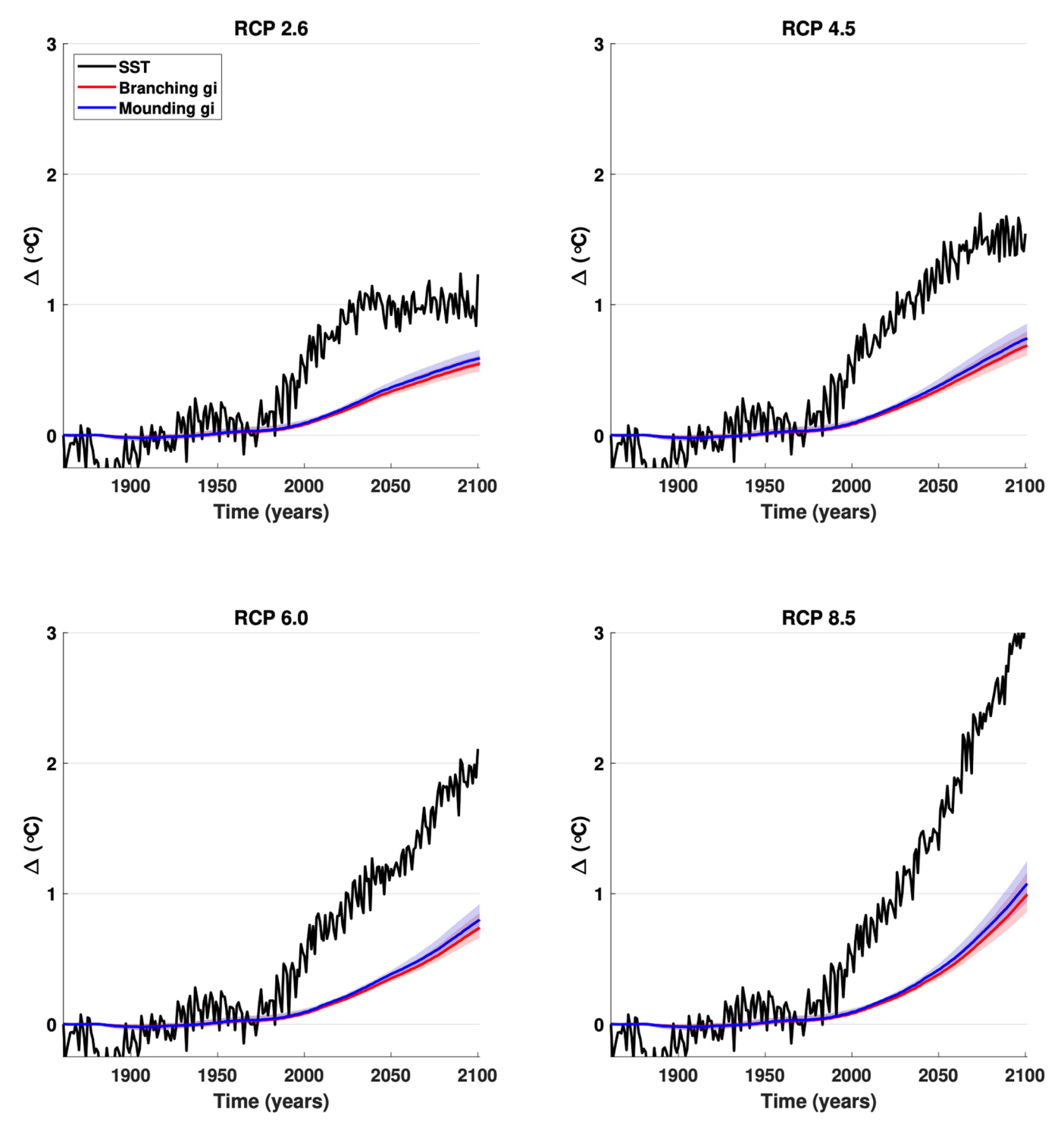
Extended Data Fig. 5 | Sensitivity analysis of percent 'healthy' coral reef cells when the model is calibrated to estimated bleaching frequencies of 3 or 5% between 1985-2010. In the main text, model output is calibrated to a 5% bleaching frequency during this time. The effect of changing the target to 3 % is shown for RCP4.5 and RCP8.5 scenarios. Projected trajectories are shown with and without symbiont evolution (E=1 vs. E=0), and with or without shuffling (+1.0 °C advantage) in the tolerant population. The effect of increasing pCO2 on coral growth rates is also included (OA=1) with evolution and shuffling.



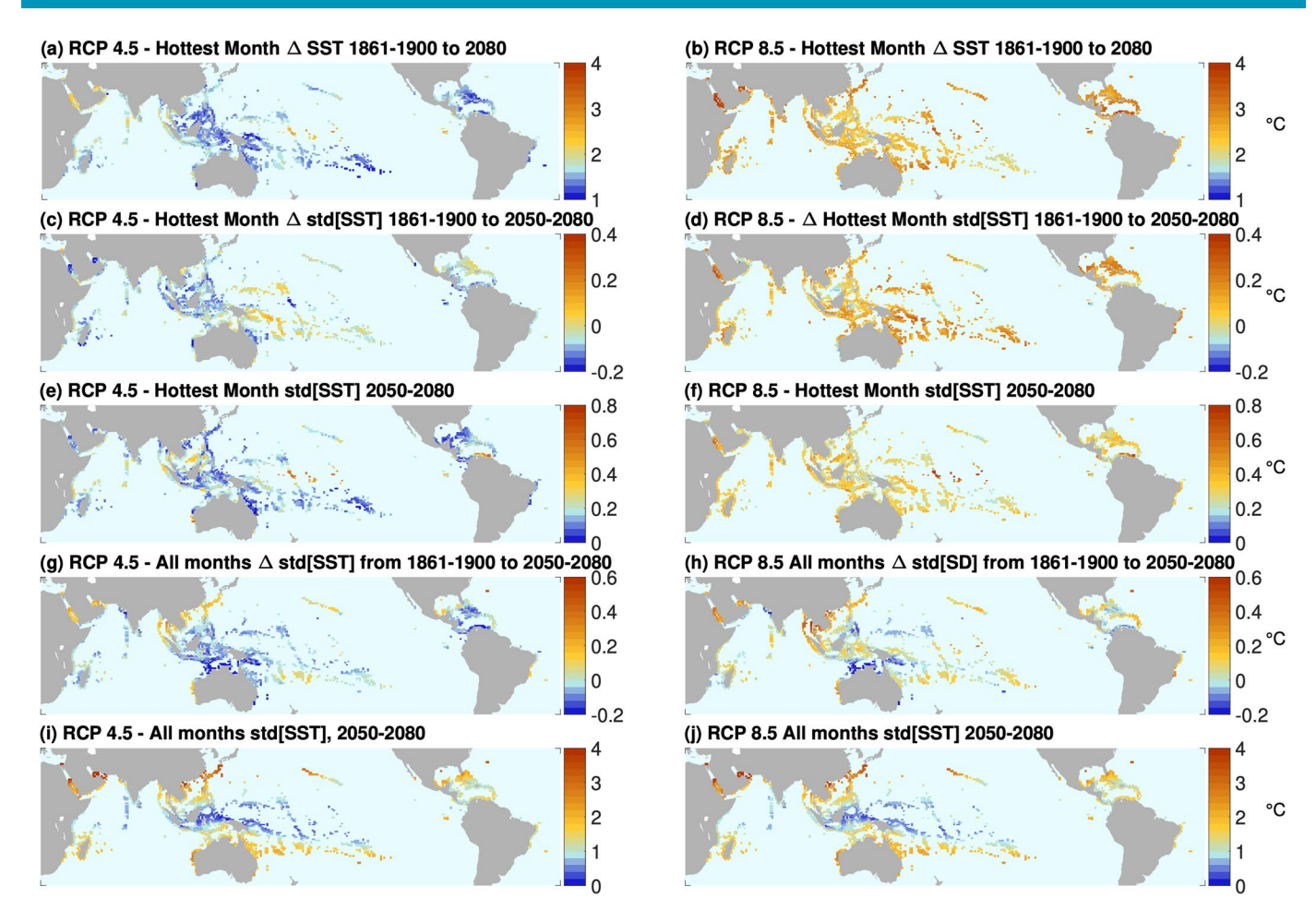
Extended Data Fig. 6 | Global mean fraction of corals hosting heat-tolerant symbionts in branching (heat-sensitive) corals and mounding (heat-tolerant) corals. The mean value is calculated for all reef cells (n=1,925) for all RCPs in shuffling (+1.0 °C advantage) simulations. For most reefs, fidelity to heat-tolerant symbiont occurs following a rapid transition between 2010-2040 through 2100.



Extended Data Fig. 7 | Fine-scale symbiont shuffling dynamics in four example reef cells. Temperature is monthly SST with the optimal temperature (gi) for each symbiont type overlaid in yellow (top). Symbiont density (bottom) is in terms of cells per cm² of coral area for a heat-sensitive (solid lines) and heat-tolerant (dashed lines) symbiont population in each coral morphotype. Realistic seasonal fluctuations in symbiont density (a,b) and reversion can occur (c, d), but reversion is uncommon under future warming; (d) represents a model run with no anthropogenic warming in which reversion occurs several times during a 200-year period. Bleaching events are shown in black circles.



Extended Data Fig. 8 | Global change in mean symbiont genotype (g_i or optimal temperature in °C) and average increase in annual maximum sea surface temperatures (SST) in model runs with symbiont evolution for all RCPs. Median (solid lines) and interquartile range (shaded) is shown across all reef cells (n=1,925) for mounding (heat-tolerant) and branching (heat-sensitive) corals. Across all RCP scenarios and all reefs, the increase in symbiont optimal thermal tolerance ranged between 0.3°C and 1.8°C.



Extended Data Fig. 9 | Global maps of warming rate and SST variability. Values represent change in each temperature metric between the historical period (1861-1900) and 2080 (a-d, g-h) as well as future variability between 2050-2080 (e-f, i-j) for RCP 4.5 and RCP 8.5 climate scenarios. In panels (a) to (f), inputs are filtered to include only maximum monthly mean SST. Panels (g) through (j) include all months.



| Corresponding author(s): | Cheryl A. Logan |
|----------------------------|-----------------|
| Last updated by author(s): | Mar 23, 2021 |

Reporting Summary

Nature Research wishes to improve the reproducibility of the work that we publish. This form provides structure for consistency and transparency in reporting. For further information on Nature Research policies, see our <u>Editorial Policies</u> and the <u>Editorial Policy Checklist</u>.

| $\overline{}$ | | 100 | | | |
|---------------|-----|-----|-----|-----|--------|
| 0 | † 2 | ١t١ | ist | ٠i. | \sim |
| | | | | | |

| For | all statistical analyses, confirm that the following items are present in the figure legend, table legend, main text, or Methods section. |
|-------------|---|
| n/a | Confirmed |
| \boxtimes | The exact sample size (n) for each experimental group/condition, given as a discrete number and unit of measurement |
| \boxtimes | A statement on whether measurements were taken from distinct samples or whether the same sample was measured repeatedly |
| \boxtimes | The statistical test(s) used AND whether they are one- or two-sided Only common tests should be described solely by name; describe more complex techniques in the Methods section. |
| \boxtimes | A description of all covariates tested |
| \boxtimes | A description of any assumptions or corrections, such as tests of normality and adjustment for multiple comparisons |
| \boxtimes | A full description of the statistical parameters including central tendency (e.g. means) or other basic estimates (e.g. regression coefficient AND variation (e.g. standard deviation) or associated estimates of uncertainty (e.g. confidence intervals) |
| \boxtimes | For null hypothesis testing, the test statistic (e.g. <i>F</i> , <i>t</i> , <i>r</i>) with confidence intervals, effect sizes, degrees of freedom and <i>P</i> value noted <i>Give P values as exact values whenever suitable.</i> |
| \boxtimes | For Bayesian analysis, information on the choice of priors and Markov chain Monte Carlo settings |
| \boxtimes | For hierarchical and complex designs, identification of the appropriate level for tests and full reporting of outcomes |
| \boxtimes | Estimates of effect sizes (e.g. Cohen's <i>d</i> , Pearson's <i>r</i>), indicating how they were calculated |
| | Our web collection on <u>statistics for biologists</u> contains articles on many of the points above. |

Software and code

Policy information about availability of computer code

Data collection

Coral reef containing grid cells were identified by projecting the Millennium Coral Reef Mapping Project (https://data.unep-wcmc.org/datasets/1) map of corals reefs to the grid used by the NOAA Geophysical Fluid Dynamics Laboratory (GFDL) Earth System Model 2M (ESM2M).

Data analysis

All code was developed and run in Matlab (R2019b; MathWorks, Natick, Massachusetts, USA). All Matlab code can be found at https://github.com/VeloSteve/Coral-Model-V12 under the following DOI: https://doi.org/10.5281/zenodo.2639126.

For manuscripts utilizing custom algorithms or software that are central to the research but not yet described in published literature, software must be made available to editors and reviewers. We strongly encourage code deposition in a community repository (e.g. GitHub). See the Nature Research guidelines for submitting code & software for further information.

Data

Policy information about <u>availability of data</u>

All manuscripts must include a data availability statement. This statement should provide the following information, where applicable:

- Accession codes, unique identifiers, or web links for publicly available datasets
- A list of figures that have associated raw data
- A description of any restrictions on data availability

All Matlab code can be found at https://github.com/VeloSteve/Coral-Model-V12 under the following DOI: https://doi.org/10.5281/zenodo.2639126.

| Field-specific | creporting | | | | | | | |
|--|---|--|--|--|--|--|--|--|
| Please select the one below that is the best fit for your research. If you are not sure, read the appropriate sections before making your selection. | | | | | | | | |
| Life sciences | Behavioural & social sciences | | | | | | | |
| For a reference copy of the document with all sections, see nature.com/documents/nr-reporting-summary-flat.pdf | | | | | | | | |
| Ecological, e | volutionary & environmental sciences study design | | | | | | | |
| All studies must disclose or | these points even when the disclosure is negative. | | | | | | | |
| Study description | We model the role of algal symbiont shuffling and symbiont evolution in coral resilience to warming and ocean acidification, globally. The model was applied to bias-corrected monthly sea surface temperature (SST) and aragonite saturation data from the NOAA-GFDL Earth System 2 Model. | | | | | | | |
| Research sample | n/a | | | | | | | |
| Sampling strategy | n/a | | | | | | | |
| Data collection | n/a | | | | | | | |
| Timing and spatial scale | n/a | | | | | | | |
| Data exclusions | n/a | | | | | | | |
| Reproducibility | n/a | | | | | | | |
| Randomization | n/a | | | | | | | |
| Blinding | n/a | | | | | | | |
| Did the study involve field | d work? Yes No | | | | | | | |
| | | | | | | | | |
| Reporting fo | r specific materials, systems and methods | | | | | | | |
| | authors about some types of materials, experimental systems and methods used in many studies. Here, indicate whether each material, evant to your study. If you are not sure if a list item applies to your research, read the appropriate section before selecting a response. | | | | | | | |
| Materials & experimental systems Methods | | | | | | | | |
| n/a Involved in the study | | | | | | | | |
| Antibodies | ChIP-seq | | | | | | | |
| Eukaryotic cell lines | | | | | | | | |
| Palaeontology and archaeology MRI-based neuroimaging MRI-based neuroimaging | | | | | | | | |
| Animals and other organisms Human research participants | | | | | | | | |
| Clinical data | | | | | | | | |
| Dual use research of concern | | | | | | | | |